

# Lyapunov Constrained Soft Actor-Critic (LC-SAC) using Koopman Operator Theory for Quadrotor Trajectory Tracking

Dhruv S. Kushwaha, *Student, IEEE*, and Zoleikha A. Biron, *Senior Member, IEEE*,

**Abstract**—Reinforcement Learning (RL) has achieved remarkable success in solving complex sequential decision-making problems. However, its application to safety-critical physical systems remains constrained by the lack of stability guarantees. Standard RL algorithms prioritize reward maximization, often yielding policies that may induce oscillations or unbounded state divergence. There has significant work in incorporating Lyapunov-based stability guarantees in RL algorithms with key challenges being selecting a candidate Lyapunov function, computational complexity by using excessive function approximators and conservative policies by incorporating stability criterion in the learning process. In this work we propose a novel Lyapunov-constrained Soft Actor-Critic (LC-SAC) algorithm using Koopman operator theory. We propose use of extended dynamic mode decomposition (EDMD) to produce a linear approximation of the system and use this approximation to derive a closed form solution for candidate Lyapunov function. This derived Lyapunov function is incorporated in the SAC algorithm to further provide guarantees for a policy that stabilizes the nonlinear system. The results are evaluated trajectory tracking of a 2D Quadrotor environment based on safe-control-gym. The proposed algorithm shows training convergence and decaying violations for Lyapunov stability criterion compared to baseline vanilla SAC algorithm. GitHub Repository: [LC-SAC-Quadrotor-Trajectory-Tracking](#).

**Index Terms**—Reinforcement Learning, Lyapunov Functions, Soft Actor-Critic, Koopman Operators, Neural Networks.

## I. INTRODUCTION

**R**EINFORCEMENT learning (RL) has emerged as a powerful approximate optimal control scheme to develop feedback policies directly from interaction data, enabling high-performance decision making in domains where first-principles modeling is difficult or where the optimal strategy is not known a priori. However, when RL controllers are deployed on physical systems (robotic manipulators, legged locomotion, aerial vehicles, energy systems) [1], stability and safety become first-order requirements because exploration-driven transients, function-approximation error, and distribution shift can lead to unstable closed-loop behavior or irreversible constraint violations [2]. This has motivated a large body of safe RL research, in which the learning objective is augmented with constraints (state/input bounds, failure avoidance, energy limits) and in which policy updates are designed to preserve feasibility throughout training and deployment.

A principled route to stability and safety is offered by Lyapunov theory, where a scalar certificate  $V(x)$  is constructed such that it decreases along trajectories, implying invariance and convergence properties of the closed-loop system. Translating this logic to RL is conceptually appealing: if policy learning can be constrained so that a Lyapunov decrease condition is satisfied, then stability-like guarantees can be enforced even while optimizing performance. Early work has proven

that Lyapunov design principles as a means to restrict learning to safe improvements and to validate learned control strategies is effective and a viable solution [3]. Many safety requirements are naturally expressed through constrained Markov decision processes (CMDPs), where one maximizes expected return subject to bounds on expected cumulative costs. Chow et al. proposed a Lyapunov-based approach for CMDPs that constructs a Lyapunov function associated with the constraint costs and then enforces local (often linearized) constraints guaranteeing global constraint satisfaction of the behavior policy during learning [4]. This viewpoint enables systematic safe versions of dynamic programming and RL updates by ensuring each update remains within a feasible set characterized by the Lyapunov function [5]. A second line of work targets stability more directly [6], [7]: the critic or a separate neural network is trained to represent a Lyapunov function, and policy improvement is constrained to satisfy a Lyapunov decrease condition (in expectation or with high probability). For example, actor-critic frameworks have been developed that embed Lyapunov stability conditions into the learning objective/constraints to guarantee closed-loop stability properties for stochastic nonlinear systems modeled as MDPs [8]. Across both approaches, the common methodology is to replace an unconstrained policy improvement step with a certificate preserving update often implemented as, (i) projection of policy parameters onto a feasible set, (ii) action projection/shielding that modifies unsafe actions, or (iii) constrained optimization where Lyapunov decrease inequalities act as constraints.

Despite their promise, Lyapunov-based RL methods face recurring limitations that constrain their applicability and the strength of their guarantees. Lyapunov function existence and construction are hard, even in classical nonlinear control, systematically constructing a valid Lyapunov function can be difficult. In RL the challenge is particularly challenging because the environment may be unknown, high-dimensional, and only accessible via samples [9]. Consequently, many approaches rely on problem structure, conservative templates, or learned approximators whose validity is difficult to certify globally. Deep RL relies on function approximation for value functions, dynamics models, and sometimes the Lyapunov certificate itself. Small approximation errors can invalidate decrease conditions or undermine the meaning of a learned certificate outside the data distribution [6], [10]. Some recent work explicitly notes sample inefficiency and practical difficulty when Lyapunov functions are learned on-policy, motivating off-policy Lyapunov learning to improve data efficiency—highlighting that certificate learning itself can become a bottleneck [10]. Furthermore, enforcing Lyapunov constraints may require solving projections or constrained

optimizations at every update or every action selection, increasing computational cost and introducing additional hyper-parameters (penalties, margins, trust-region sizes) [11], [12].

To address these challenges we propose a Lyapunov-constrained SAC algorithm that uses Koopman Operator theory to obtain an offline closed form solution for a candidate control Lyapunov function (CLF). We learn a linear dynamical system using EDMD and solve the Algebraic Riccati Equation (ARE) to obtain a closed form solution for the CLF. The derived CLF guarantees the existence and reduces the computational complexity of incorporating stability in safe RL. We further propose a Lyapunov-constrained SAC (LC-SAC) algorithm to incorporate the Lyapunov stability criteria in policy loss function and provide analysis for satisfying the stability criterion. **The main contributions of this work are as follows:**

1. **We propose a novel methodology to obtain closed form solution for CLF and incorporate it in SAC algorithm.**
2. **Analysis for effect on augmenting the policy loss in SAC by the Lyapunov constraint term.**

The rest of the paper is organized as follows, Section **II** briefly covers the notation and theoretical background for further discussion, Section **III** covers the proposed Lyapunov-constrained SAC algorithm and its analysis. Section **IV** provides details on experimental setup and Section **V** covers the discussion on results conducted on 2D Quadrotor trajectory tracking. Finally, Section **VI** discusses conclusions of this work and future research directions.

## II. THEORETICAL BACKGROUND

Some formal definitions and notations are described in this section to give the reader context for further discussion. The theory is kept brief and sources for detailed explanations are cited.

### A. Lyapunov Functions (Discrete-Time)

*Theorem 1:* [13] Consider a discrete-time closed-loop system

$$x(k+1) = f_{cl}(x(k)), \quad (1)$$

with desired (equilibrium) state  $x_d \in \mathcal{X}$ . A continuously differentiable function  $V : \mathcal{X} \rightarrow \mathbb{R}$  is a (discrete-time) Lyapunov function if:

$$V(x_d) = 0 \quad (2a)$$

$$V(x) > 0, \quad \forall x \in \mathcal{X} \setminus \{x_d\} \quad (2b)$$

$$V(x(k+1)) - V(x(k)) \leq 0, \quad \forall x(k) \in \mathcal{X} \quad (2c)$$

Similarly, to satisfy conditions for exponential stability in discrete time [13], the first two conditions (2a)–(2b) remain the same, except the Lyapunov decrease condition is strengthened to

$$V(x(k+1)) - V(x(k)) \leq -\eta V(x(k)), \quad \eta \in (0, 1) \quad (3)$$

Equivalently, (3) implies the contraction form  $V(x(k+1)) \leq (1 - \eta)V(x(k))$ , which ensures geometric decay of  $V$  and hence exponential convergence to  $x_d$ .

The underlying concept behind (2a)–(2b) is that the Lyapunov function  $V$  can be interpreted as an energy-like measure that is zero at the equilibrium  $x_d$  and increases as the state moves away from it. Condition (2c) requires that this “energy” does not increase from one time step to the next; instead, it either remains constant or decreases. The strengthened condition (3) enforces a strict decrease proportional to the current energy level, yielding exponential stability.

*a) Discrete-Time Control Lyapunov Functions.:* Control Lyapunov functions (CLFs) can be used to provide guarantees for stabilizability of a controlled system, i.e., existence of a feedback policy that renders the closed-loop system stable. The notion of CLFs can be extended to discrete-time control systems in a manner analogous to the continuous-time case [14].

*Theorem 2:* Consider a discrete-time control system

$$x(k+1) = f(x(k), u(k)), \quad (4)$$

with admissible control set  $\mathcal{U}$  and desired state  $x_d \in \mathcal{X}$ . A CLF  $V$  is a smooth, proper and positive definite function

$$V : \mathbb{R}^n \rightarrow \mathbb{R}, \quad (5)$$

that certifies asymptotic stabilizability about  $x_d$  if:

$$V(x_d) = 0 \quad (6a)$$

$$V(x) > 0, \quad \forall x \in \mathcal{X} \setminus \{x_d\} \quad (6b)$$

$$\inf_{u \in \mathcal{U}} [V(f(x, u)) - V(x)] \leq 0, \quad \forall x \in \mathcal{X} \quad (6c)$$

Similarly, for exponential stabilizability about  $x_d$ , the first two conditions (6a)–(6b) remain the same, while the decrease condition is modified to

$$\inf_{u \in \mathcal{U}} [V(f(x, u)) - V(x) + \eta V(x)] \leq 0, \quad \forall x \in \mathcal{X}, \quad \eta \in (0, 1) \quad (7)$$

Equivalently, (7) implies the existence of a control input such that  $V(f(x, u)) \leq (1 - \eta)V(x)$ .

Thus, any Lipschitz policy  $\pi(x)$  that chooses  $u = \pi(x)$  satisfying (6c) and (7) will necessarily provide asymptotic and exponential stability for the discrete-time system, respectively.

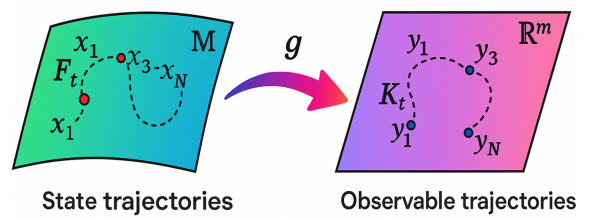


Fig. 1. Koopman Operator: State trajectories  $x_t$  and observable trajectories  $y_t := g(x_t)$ .

### B. Soft Actor-Critic Algorithm

A Markov Decision Process (MDP) can be denoted by the tuple  $\langle \mathcal{S}, \mathcal{A}, \mathcal{R}, \mathbb{P}, \mu, \gamma \rangle$  [15], where  $\mathcal{S}$  and  $\mathcal{A}$  denote the set of states and actions, respectively.  $\mathcal{R} : \mathcal{S} \times \mathcal{A} \times \mathcal{S} \mapsto \mathbb{R}$  denotes the reward function,  $\mathbb{P} : \mathcal{S} \times \mathcal{A} \times \mathcal{S} \mapsto [0, 1]$  denotes the transition probability function,  $\mu : \mathcal{S} \mapsto [0, 1]$  is the initial

probability distribution and  $\gamma$  denotes the discount factor for future rewards. A policy  $\pi : \mathcal{S} \mapsto \mathcal{P}(A)$  is a mapping from states to a probability distribution over actions and  $\pi(a_t|s_t)$  is the probability of taking action  $a$  under state  $s$  at time  $t$ .

Soft Actor-Critic (SAC) is an off-policy, actor-critic Deep Reinforcement Learning (DRL) algorithm based on the maximum entropy reinforcement learning framework [16]. Unlike standard RL, which aims solely to maximize the expected sum of rewards, SAC maximizes a weighted objective of reward and policy entropy. This approach encourages exploration and provides robustness to sample brittleness and hyperparameter settings. The central feature of SAC is the entropy-augmented objective function. The agent aims to learn a policy  $\pi(a_t|s_t)$  that maximizes both the expected return and entropy of the policy  $\mathcal{H}(\pi(\cdot|s_t))$ . The objective, denoted as  $J(\pi)$ , is defined as:

$$J(\pi) = \sum_{t=0}^T \mathbb{E}_{(s_t, a_t) \sim \rho_\pi} [r(s_t, a_t) + \alpha \mathcal{H}(\pi(\cdot|s_t))]$$

where,  $\rho_\pi$  is the trajectory distribution induced by policy  $\pi$ .  $\mathcal{H}(\pi(\cdot|s_t)) = -\mathbb{E}_{a \sim \pi} [\log \pi(a|s_t)]$  is the entropy of policy at state  $s_t$ .  $\alpha$  is the temperature parameter determining the relative importance of the entropy term against the reward.

The critic estimates the soft Q-value, which describes the value of taking action  $a_t$  in state  $s_t$  and following the optimal entropy-maximizing policy. The soft Q-function parameters  $\theta$  are trained to minimize the soft Bellman residual:

$$J_Q(\theta) = \mathbb{E}_{(s_t, a_t) \sim \mathcal{D}} \left[ \frac{1}{2} (Q_\theta(s_t, a_t) - y_t)^2 \right] \quad (8)$$

The target value  $y_t$  incorporates the entropy term implicitly via the soft value function:

$$y_t = r(s_t, a_t) + \gamma \mathbb{E}_{s_{t+1} \sim p} \left[ \min_{j=1,2} Q_{\theta_j}(s_{t+1}, a_{t+1}) - \alpha \log \pi_\phi(a_{t+1}|s_{t+1}) \right] \quad (9)$$

Note: SAC typically employs "Clipped Double-Q Learning" [17] (using two critics,  $Q_{\theta_1}$  and  $Q_{\theta_2}$ ) to mitigate positive bias, taking the minimum Q-value for the target computation. The actor updates the policy parameters  $\phi$  by minimizing the Kullback-Leibler (KL) divergence between the policy and exponential of the soft Q-function. To allow gradients to backpropagate through the stochastic sampling process, SAC utilizes the reparameterization trick. The action is sampled using a differentiable transformation of noise:

$$a_t = f_\phi(\epsilon_t; s_t) = \tanh(\mu_\phi(s_t) + \sigma_\phi(s_t) \cdot \epsilon_t), \quad (10)$$

$$\epsilon_t \sim \mathcal{N}(0, I) \quad (11)$$

The policy objective function is then minimized as follows:

$$J_\pi(\phi) = \mathbb{E}_{s_t \sim \mathcal{D}, \epsilon_t \sim \mathcal{N}} [\alpha \log \pi_\phi(f_\phi(\epsilon_t; s_t)|s_t) - \min_{j=1,2} Q_{\theta_j}(s_t, f_\phi(\epsilon_t; s_t))] \quad (12)$$

Finally, Rather than fixing the temperature  $\alpha$  as a static hyperparameter, modern implementations treat  $\alpha$  as a learnable

parameter. It is adjusted to maintain a minimum target entropy  $\bar{\mathcal{H}}$ , effectively constraining the exploration capability:

$$J(\alpha) = \mathbb{E}_{a_t \sim \pi_t} [-\alpha (\log \pi_t(a_t|s_t) + \bar{\mathcal{H}})] \quad (13)$$

Soft Actor-Critic combines (i) maximum-entropy RL for robust exploration, (ii) off-policy learning with a replay buffer for sample efficiency, (iii) stochastic actor updates using reparameterization, and (iv) twin critics with min-targets for stability.

### C. Koopman Operator Theory

Koopman operator theory provides a global linearization framework for nonlinear dynamical systems. Unlike local linearization techniques (e.g., Jacobian linearization near equilibrium points), this theoretic framework lifts the state-space dynamics into an infinite-dimensional Hilbert space of observable functions, where the evolution is linear [18]. Consider a discrete-time dynamical system evolving on a state space manifold  $\mathcal{M} \subseteq \mathbb{R}^n$ :

$$x_{k+1} = F(x_k) \quad (14)$$

We define a Hilbert space of scalar-valued observable functions  $g : \mathcal{M} \rightarrow \mathbb{C}$ , denoted as  $\mathcal{H}$ . The Koopman operator  $\mathcal{K} : \mathcal{H} \rightarrow \mathcal{H}$  is an infinite-dimensional linear operator that acts on these observables by composing them with the dynamics  $F$ :

$$\mathcal{K}g(x_k) = g(F(x_k)) = g(x_{k+1}) \quad (15)$$

Crucially, while the underlying dynamics  $F$  may be nonlinear, the operator  $\mathcal{K}$  is linear by definition:

$$\mathcal{K}(\alpha g_1 + \beta g_2) = \alpha \mathcal{K}g_1 + \beta \mathcal{K}g_2, \quad \forall \alpha, \beta \in \mathbb{C} \quad (16)$$

The behavior of a nonlinear system is characterized by the spectral properties of  $\mathcal{K}$ . If  $\mathcal{K}$  admits a spectral decomposition, the evolution of an observable  $g(x)$  can be expanded in terms of the Koopman eigenfunctions  $\varphi_j(x)$  and eigenvalues  $\mu_j$ :

$$\mathcal{K}\varphi_j(x) = \mu_j \varphi_j(x) \quad (17)$$

The evolution of observable  $g(x)$  from time  $k = 0$  is then given by:

$$g(x_k) = \mathcal{K}^k g(x_0) = \sum_{j=1}^{\infty} v_j \mu_j^k \varphi_j(x_0) \quad (18)$$

where  $v_j$  are the Koopman modes, representing the projection of observable  $g$  onto the eigenfunctions.

Since the Koopman operator is infinite-dimensional, practical implementation requires a finite-dimensional approximation. Extended Dynamic Mode Decomposition (EDMD) is a data-driven algorithm that approximates  $\mathcal{K}$  by restricting it to a finite subspace spanned by a user-defined dictionary of observables [19]. We define a dictionary of  $N$  basis functions (observables)  $\Psi(x) = [\psi_1(x), \psi_2(x), \dots, \psi_N(x)]^T$ . The EDMD algorithm seeks a matrix  $\mathbf{K} \in \mathbb{R}^{N \times N}$  that approximates the action of the Koopman operator on this subspace [18], [19]:

$$\mathcal{K}\Psi(x) \approx \mathbf{K}^T \Psi(x) \quad (19)$$

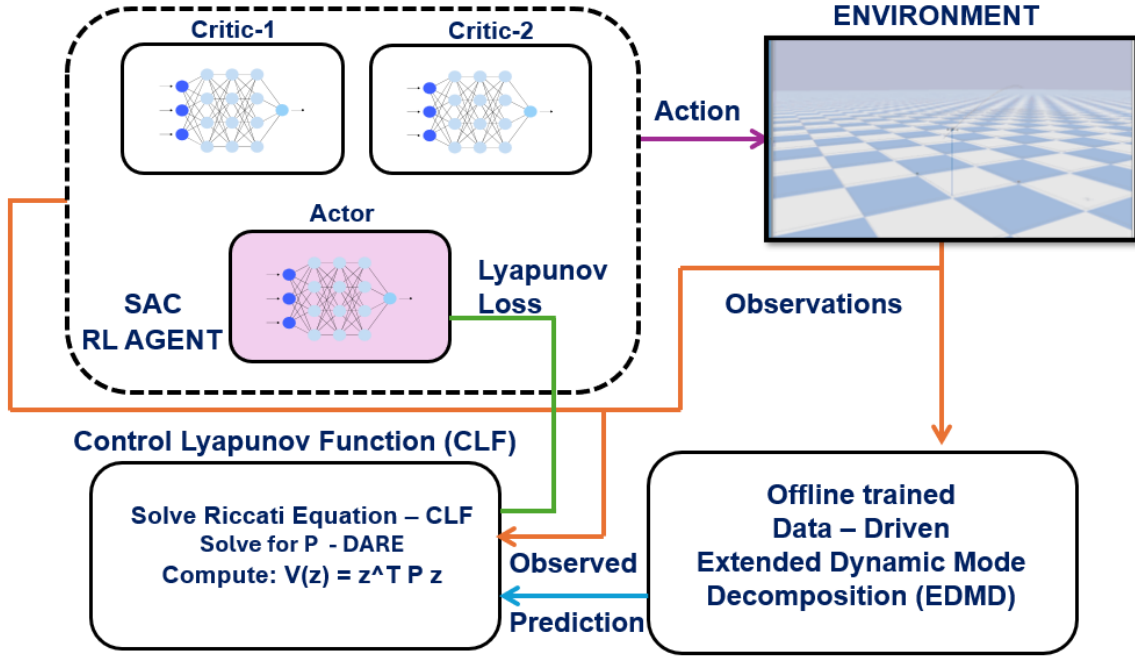


Fig. 2. Proposed methodology for Lyapunov-based SAC.

Given a dataset of  $M$  snapshot pairs  $\{(x_i, y_i)\}_{i=1}^M$  where  $y_i = F(x_i)$ , we construct two data matrices by evaluating the dictionary on the snapshots:

$$\Psi_X = [\Psi(x_1), \dots, \Psi(x_M)], \quad \Psi_Y = [\Psi(y_1), \dots, \Psi(y_M)] \quad (20)$$

The finite-dimensional approximation  $\mathbf{K}$  is obtained by minimizing the Frobenius norm of the residual of linear prediction in the lifted space:

$$\min_{\mathbf{K}} \|\Psi_Y - \mathbf{K}^T \Psi_X\|_F^2 \quad (21)$$

The optimal solution to the least-squares problem is given formally by:

$$\mathbf{K}^T = \Psi_Y \Psi_X^\dagger \quad (22)$$

where  $\Psi_X^\dagger$  denotes the Moore-Penrose pseudoinverse [20]. In practice, this is often computed using the matrices  $G = \frac{1}{M} \Psi_X \Psi_X^T$  and  $A = \frac{1}{M} \Psi_X \Psi_Y^T$ , such that:

$$\mathbf{K}^T = AG^\dagger \quad (23)$$

The eigenvalues of  $\mathbf{K}$  approximate the Koopman eigenvalues  $\mu_j$ , and the eigenvectors of  $\mathbf{K}$  are used to reconstruct the Koopman eigenfunctions.

### III. PROPOSED METHODOLOGY

The proposed methodology follows Algorithm 1 and is divided into three parts:

- Offline approximation of discrete-time control-affine dynamics in a lifted space using EDMD.
- Closed-form candidate CLF construction by solving the Discrete Algebraic Riccati Equation (DARE).

- Online SAC policy optimization with a Lyapunov constraint enforced via a Lagrangian penalty.

*Offline Model Learning & CLF Derivation:* We use Koopman operator theory to approximate nonlinear dynamics by a linear control-affine model in a lifted coordinate system. Extended Dynamic Mode Decomposition (EDMD), discussed in Section II-C, is used to learn the lifted mapping  $g(\cdot)$  and the corresponding system matrices in a purely data-driven manner. Let the lifting be defined by a vector of basis functions  $g : \mathbb{R}^n \rightarrow \mathbb{R}^N$ , with lifted state  $z = g(x)$ . Using a dataset of state transitions collected from a random or baseline policy, EDMD identifies a discrete-time lifted model of the form

$$z_{t+1} \approx Az_t + Bu_t, \quad (24)$$

where  $A \in \mathbb{R}^{N \times N}$  and  $B \in \mathbb{R}^{N \times m}$ . This model acts as a surrogate for the true nonlinear dynamics in the lifted space, while preserving a control-affine structure in  $u$  [21], [22]. When needed, an approximation of the state in the original space can be recovered through a projection matrix  $C$ , i.e.,  $\hat{x}_t = Cz_t$ .

Using  $(A, B)$ , we derive a closed-form quadratic candidate CLF by solving the discrete-time infinite-horizon LQR problem

$$J = \sum_{t=0}^{\infty} (z_t^T Q z_t + u_t^T R u_t), \quad (25)$$

where  $Q \succeq 0$  and  $R \succ 0$ . Under standard stabilizability/detectability conditions, the DARE admits a unique stabilizing solution  $P \succeq 0$  [23], [24]:

$$P = A^T P A - A^T P B (R + B^T P B)^{-1} B^T P A + Q \quad (26)$$

We then define the closed-form candidate CLF

$$V(x) = V(z) = z^T P z, \quad z = g(x) \quad (27)$$

This derivation avoids training an auxiliary Lyapunov network, reduces computational complexity, and yields a structured CLF whose decrease can be evaluated efficiently during online learning.

*Online Policy Optimization with Lyapunov Constraint:* During online training, the agent interacts with the environment and stores transitions  $(x_t, u_t, r_t, x_{t+1}, d_t)$  in a replay buffer  $\mathcal{D}$ . When the update condition is met, a mini-batch  $B = \{(x, u, r, x', d)\}$  is sampled from  $\mathcal{D}$  and the critic and actor are updated.

*a) Critic update (standard SAC):* For each sampled transition, we sample  $u' \sim \pi_\theta(\cdot|x')$  and form the SAC target

$$Q_{\text{target}} = r + \gamma(1-d) \left( \min_{j=1,2} Q_{\bar{\phi}_j}(x', u') - \alpha \log \pi_\theta(u'|x') \right) \quad (28)$$

Each critic  $Q_{\phi_j}$  is updated by minimizing the mean-squared Bellman error:

$$L_Q(\phi_j) = \frac{1}{|B|} \sum_{(x, u, r, x', d) \in B} (Q_{\phi_j}(x, u) - Q_{\text{target}})^2 \quad (29)$$

*b) Actor update (Lyapunov constrained, Lagrangian form):* The actor is updated using the reparameterization trick by sampling  $\tilde{u} \sim \pi_\theta(\cdot|x)$  and computing the standard SAC objective

$$\mathcal{J}_{\text{SAC}}(x, \tilde{u}) = - \min_{j=1,2} Q_{\phi_j}(x, \tilde{u}) + \alpha \log \pi_\theta(\tilde{u}|x) \quad (30)$$

To enforce stability, we evaluate a one-step Lyapunov decrease surrogate using the EDMD model. For each  $x$  in the batch, we compute  $z = g(x)$  and the predicted next lifted state

$$z_{\text{next}} = Az + Bu \quad (31)$$

We then compute  $V(z) = z^T P z$  and  $V(z_{\text{next}}) = z_{\text{next}}^T P z_{\text{next}}$ , and define the violation term exactly as in Algorithm 1:

$$\mathcal{L}_v(x, \tilde{u}) = \max(V(z_{\text{next}}) - V(z) + \eta V(z), 0), \quad (32)$$

where  $a > 0$  is a stability decay coefficient and  $\max(\cdot, 0)$  ensures that the penalty is active only when the decrease condition is violated. Note that (32) enforces the discrete-time inequality

$$V(z_{\text{next}}) - V(z) \leq -\eta V(z), \quad (33)$$

which is a sufficient decrease condition implying contraction in a quadratic norm induced by  $P$  when  $P \succ 0$ .

We incorporate this constraint using a Lagrangian relaxation with multiplier  $\lambda \geq 0$  and tolerance  $\zeta > 0$  [25]. The actor loss is

$$\mathcal{L}_\pi(\theta) = \frac{1}{|B|} \sum_{x \in B} [\mathcal{J}_{\text{SAC}}(x, \tilde{u}) + \lambda(\mathcal{L}_v(x, \tilde{u}) - \zeta)] \quad (34)$$

The multiplier is updated via projected ascent:

$$\lambda \leftarrow \max \left( 0, \lambda + \beta_\lambda \left( \frac{1}{|B|} \sum_{x \in B} \mathcal{L}_v(x, \tilde{u}) - \zeta \right) \right) \quad (35)$$

Finally, the temperature  $\alpha$  is updated toward a target entropy, and the target critics are updated using Polyak averaging:

$$\bar{\phi}_j \leftarrow \tau \phi_j + (1 - \tau) \bar{\phi}_j \quad (36)$$

### A. Stability Analysis

We analyze how the Lyapunov-constrained actor update in Algorithm 1 enforces a one-step decrease condition for the *surrogate* (EDMD) lifted dynamics and hence induces exponential stability of the lifted closed-loop system when the constraint is satisfied.

*a) Surrogate dynamics and CLF:* Let the lifted state be  $z = g(x) \in \mathbb{R}^N$  and consider the EDMD surrogate model

$$z_{t+1} = Az_t + Bu_t \quad (37)$$

Let  $P \succ 0$  be the stabilizing solution of the DARE (26) and define the quadratic candidate CLF

$$V(z) = z^T P z \quad (38)$$

Assume  $\pi_\theta : \mathbb{R}^n \rightarrow \mathbb{R}^m$  is locally Lipschitz and define the lifted closed-loop map

$$F_\theta(z) := Az + B\pi_\theta(x), \quad \text{x s.t. } z = g(x) \quad (39)$$

(For the proof below, it is sufficient to consider  $z$  as the state and  $u = \pi_\theta(\cdot)$  as a feedback law producing  $u_t$ .)

*b) Constraint enforced by LC-SAC:* Algorithm 1 defines the hinge violation

$$\mathcal{L}_v(z, u) = \max(s(z, u), 0), \quad (40)$$

$$s(z, u) := V(Az + Bu) - V(z) + \eta V(z), \quad (41)$$

and aims to keep  $\mathbb{E}[\mathcal{L}_v] \leq \zeta$  by minimizing the primal objective and ascending in the dual variable  $\lambda \geq 0$ . Ignoring sampling noise and function approximation error, the *pointwise* satisfaction of  $s(z, \pi_\theta) \leq 0$  implies the discrete decrease condition

$$V(z_{t+1}) - V(z_t) \leq -\eta V(z_t) \quad (42)$$

*c) From (42) to exponential stability (lifted system):* Since  $P \succ 0$ , there exist constants  $m_1, m_2 > 0$  such that for all  $z$ ,

$$m_1 \|z\|^2 \leq V(z) \leq m_2 \|z\|^2, \\ m_1 = \lambda_{\min}(P), \quad m_2 = \lambda_{\max}(P)$$

Using the upper bound  $\|z\|^2 \geq \frac{1}{m_2} V(z)$  in (42) yields

$$V(z_{t+1}) \leq V(z_t) - a \|z_t\|^2 \leq V(z_t) - \frac{a}{m_2} V(z_t) \\ = \left( 1 - \frac{a}{m_2} \right) V(z_t) \quad (43)$$

If  $0 < a < m_2$ , define  $\eta := \frac{a}{m_2} \in (0, 1)$ . Iterating (43) gives

$$V(z_t) \leq (1 - \eta)^t V(z_0) \quad (44)$$

Finally, combining (44) with the lower bound in (43) yields

$$\|z_t\|^2 \leq \frac{1}{m_1} V(z_t) \leq \frac{1}{m_1} (1 - \eta)^t V(z_0) \leq \frac{m_2}{m_1} (1 - \eta)^t \|z_0\|^2, \quad (45)$$

i.e.,

$$\|z_t\| \leq \sqrt{\frac{m_2}{m_1}} (1 - \eta)^{t/2} \|z_0\| \quad (46)$$

Thus, if the policy enforces the one-step inequality (42) for all  $z$  in a region of interest, then the lifted closed-loop surrogate system is exponentially stable in that region.

*d) How the LC-SAC updates reduce violation:* We now show that the actor update in Algorithm 1 moves parameters in a direction that *decreases* the violation score  $s(z, \pi_\theta)$  whenever the constraint is active.

Fix a sample  $z$  and let  $u_\theta$  denote the re-parameterized action output used for backpropagation. Define the sample-wise constrained actor objective (ignoring the SAC term for the moment)

$$\ell_\theta(z) := \lambda(\max(s(z, u_\theta), 0) - \zeta) \quad (47)$$

In the violation regime  $s(z, u_\theta) > 0$ , the hinge is differentiable and

$$\nabla_\theta \ell_\theta(z) = \lambda \nabla_\theta s(z, u_\theta) \quad (48)$$

Since  $z_{\text{next}} = Az + Bu_\theta$  and  $V(z) = z^\top Pz$ , we have

$$\nabla_u s(z, u) = \nabla_u V(Az + Bu) = 2B^\top P(Az + Bu), \quad (49)$$

and therefore (by the chain rule)

$$\begin{aligned} \nabla_\theta s(z, u_\theta) &= \left( \nabla_u s(z, u) \Big|_{u=u_\theta} \right)^\top \nabla_\theta u_\theta \\ &= (2B^\top P z_{\text{next}})^\top \nabla_\theta u_\theta \end{aligned} \quad (50)$$

Consider a gradient descent step on  $\theta$  with step size  $\beta_\pi$ :

$$\theta^+ = \theta - \beta_\pi \nabla_\theta \ell_\theta(z) = \theta - \beta_\pi \lambda \nabla_\theta s(z, u_\theta) \quad (51)$$

where,  $s(z, u_\theta) > 0$ . A first-order Taylor expansion of  $s$  around  $\theta$  gives

$$\begin{aligned} s(z, u_{\theta^+}) &\approx s(z, u_\theta) + \nabla_\theta s(z, u_\theta)^\top (\theta^+ - \theta) \\ &= s(z, u_\theta) - \beta_\pi \lambda \|\nabla_\theta s(z, u_\theta)\|^2 \end{aligned} \quad (52)$$

Hence,

$$s(z, u_{\theta^+}) \leq s(z, u_\theta) \quad \text{whenever } s(z, u_\theta) > 0, \lambda > 0, \quad (53)$$

with strict decrease whenever  $\nabla_\theta s(z, u_\theta) \neq 0$ . Therefore, the stability term in the actor update provably reduces the one-step Lyapunov violation score locally, pushing the policy toward satisfaction of (42).

*e) Dual update enforces constraint on average:* Define the batch-averaged constraint function

$$g(\theta) := \frac{1}{|B|} \sum_{z \in B} \mathcal{L}_v(z, u_\theta) - \zeta \quad (54)$$

Algorithm 1 performs projected dual ascent

$$\lambda^+ = \Pi_{\mathbb{R}_{\geq 0}}(\lambda + \beta_\lambda g(\theta)), \quad (55)$$

which increases  $\lambda$  when  $g(\theta) > 0$  (average violation above tolerance) and decreases it otherwise (through projection), thus adaptively strengthening or relaxing constraint pressure. Under standard primal-dual conditions (convexity and suitable step sizes), iterates converge to a KKT point of the constrained problem; while the deep RL setting is non-convex, (55) still provides a principled mechanism that drives the empirical constraint toward feasibility.

*f) Safe regime and non-interference:* If  $s(z, u_\theta) \leq 0$ , then  $\mathcal{L}_v(z, u_\theta) = 0$  and  $\nabla_\theta \mathcal{L}_v = 0$  at that sample, so the actor gradient reduces to the standard SAC gradient. Thus, the Lyapunov term does not affect reward maximization in regions where the sufficient decrease condition already holds.

*g) Remark (model mismatch):* The stability statement (46) holds for the EDMD surrogate dynamics. For the true nonlinear system, an additional approximation-error analysis is required to translate surrogate decrease into true decrease; nevertheless, the proposed algorithm guarantees that learning updates act to decrease the surrogate Lyapunov violation, and whenever (42) is satisfied (e.g., empirically over a region), exponential stability of the lifted surrogate closed-loop follows directly.

*h) Remark (Error-State Formulation in EDMD and Lyapunov Analysis):* In this work, the state used for EDMD identification and Lyapunov evaluation is the *tracking error* rather than the raw state. Specifically, we define the error state

$$e_t := x_t - x_{\text{ref},t}, \quad (56)$$

and construct the lifted coordinates using  $z_t = g(e_t)$ , yielding the surrogate lifted dynamics

$$z_{t+1} \approx Az_t + Bu_t, \quad z_t = g(e_t) \quad (57)$$

Accordingly, the candidate CLF is evaluated on the error,

$$V(e_t) = z_t^\top P z_t = g(e_t)^\top Pg(e_t), \quad (58)$$

and the Lyapunov decrease constraint is imposed on the evolution of  $e_t$ .

This error-state formulation is adopted for two reasons. First, the stabilizing objective in trajectory tracking is convergence to the reference, i.e.,  $x_t \rightarrow x_{\text{ref},t}$ , which is equivalently  $e_t \rightarrow 0$ . Hence, a Lyapunov function defined on  $e$  naturally certifies tracking stability about the origin in error coordinates and avoids ambiguity about the equilibrium point when  $x_{\text{ref},t}$  is time-varying. Second, when EDMD is learned on the error state, the identified linear surrogate captures *local incremental dynamics* around the reference, which typically improves model accuracy within the region relevant for control, reduces the effective nonlinearity seen by the lifting, and yields a more meaningful quadratic CLF via the DARE (since  $V(e) = 0$  at the desired tracking condition  $e = 0$ ). In particular, learning  $A, B$  for  $e$  aligns the surrogate model and the Lyapunov constraint with the closed-loop goal (error contraction), whereas using the absolute state  $x$  would generally require redefining the Lyapunov equilibrium at  $x_{\text{ref},t}$  and would conflate regulation about a moving operating point with global state dynamics.

#### IV. EXPERIMENTAL SETUP

To evaluate the proposed Lyapunov-Constrained Soft Actor-Critic (LC-SAC) algorithm, we conducted experiments on a high-fidelity 2D quadrotor simulation. The experimental framework is divided into three components: (i) The simulation environment - `safe-control-gym`, (ii) Koopman operator approximation using `PyKoopman`, and (iii) Implementation details of the reinforcement learning agents using `PyTorch`.

**Simulation Environment:** We utilize the safety-control-gym benchmark suite [26] for the 2D Quadrotor Trajectory Tracking task. This environment simulates the non-linear dynamics

**Algorithm 1** Lyapunov-Constrained Soft Actor-Critic (LC-SAC) with EDMD

**Require:** Initial policy parameters  $\theta$ , Critic parameters  $\phi_1, \phi_2$ , Target parameters  $\bar{\phi}_1, \bar{\phi}_2$ .

**Require:** Replay buffer  $\mathcal{D}$ , Learning rates  $\beta_\pi, \beta_Q, \beta_\alpha$ .

**Require:** Hyperparameters: tolerance for  $\mathcal{L}_\lambda$ :  $\zeta$ , Stability decay rate  $a$ , Target smoothing  $\tau$ , discount factor  $\gamma$ , temperature coefficient  $\alpha$ .

**Offline Model Learning & CLF Derivation**

Collect dataset of state transitions using a baseline PID policy.

State for EDMD  $e := x - x_{\text{ref}}$ .

Train EDMD to obtain basis functions  $g(e)$  and system matrices  $A, B$  (Eq. 2).

Solve Discrete Algebraic Riccati Equation using  $(A, B)$  to obtain matrix  $P$  (Eq. 5).

Define Closed-Form CLF:  $V(e) = g(e)^T P g(e)$ .

**Online Policy Optimization**

**for** each environment step **do**

Observe state  $x_t$  and sample action  $u_t \sim \pi_\theta(\cdot|x_t)$ .

Execute  $u_t$ , observe reward  $r_t$ , next state  $x_{t+1}$ , and done signal  $d_t$ .

Store transition  $(x_t, u_t, r_t, x_{t+1}, d_t)$  in  $\mathcal{D}$ .

**if** Update Condition Met **then**

Sample mini-batch of transitions  $B = \{(x, u, r, x', d)\}$  from  $\mathcal{D}$ .

**1. Critic Update (Standard SAC)**

Sample  $u' \sim \pi_\theta(\cdot|x')$ .

Compute target:

$$Q_{\text{target}} = r + \gamma(1 - d)(\min_{j=1,2} Q_{\bar{\phi}_j}(x', u') - \alpha \log \pi_\theta(u'|x'))$$

Update Critics  $\phi_j$  by minimizing:

$$L_Q(\phi_j) = \frac{1}{|B|} \sum (Q_{\phi_j}(x, u) - Q_{\text{target}})^2.$$

**2. Actor Update (Lyapunov Constrained)**

Sample actions  $\tilde{u} \sim \pi_\theta(\cdot|x)$  using reparameterization trick.

Compute SAC objective:

$$\mathcal{J}_{\text{SAC}} = -\min_{j=1,2} Q_{\phi_j}(x, \tilde{u}) + \alpha \log \pi_\theta(\tilde{u}|x).$$

Compute Lyapunov derivative using EDMD model:

Compute  $e = x - x_{\text{ref}}$

Lifted state  $z = g(e)$ , Derivative  $z_{\text{next}} = Az + B\tilde{u}$

$$V(z) = z^T P z, \quad V(z_{\text{next}}) = z_{\text{next}}^T P z_{\text{next}}$$

Compute Violation (Eq. (32)):

$$\mathcal{L}_v(x, \tilde{u}) = \max(V(z_{\text{next}}) - V(z) + \eta V(z), 0).$$

Update Actor  $\theta$  by minimizing total loss:

$$\mathcal{L}_\pi(\theta) = \frac{1}{|B|} \sum [\mathcal{J}_{\text{SAC}} + \lambda(\mathcal{L}_v(x, \tilde{u}) - \zeta)].$$

Update Lagrange Multiplier  $\lambda$ :

$$\lambda \leftarrow \max \left( 0, \lambda + \beta_\lambda \left( \frac{1}{|B|} \sum \mathcal{L}_v(x, \tilde{u}) - \zeta \right) \right)$$

**3. Update Hyperparameter**

Update temperature  $\alpha$  against target entropy.

Update target networks:  $\bar{\phi}_j \leftarrow \tau \phi_j + (1 - \tau) \bar{\phi}_j$ .

**end if**

**end for**

of a quadrotor subject to physical constraints and actuation limits. The quadrotor state space is defined as  $x = [p, v, \phi, \omega]^T \in \mathbb{R}^6$ , consisting of position  $p \in \mathbb{R}^2$ , linear velocity  $v \in \mathbb{R}^2$ , Euler angles  $\phi \in \mathbb{R}^2$  (roll, pitch, yaw), and angular body rates  $\omega \in \mathbb{R}^2$  in the XZ coordinate frame. The action space  $u \in \mathbb{R}^2$  corresponds to the normalized thrust commands for the four rotors. The objective is to track a reference trajectory (figure-8, circle and square) while minimizing tracking error and control effort. The reward  $r_t$  is defined as a function of the position error  $e_p = \|p_{\text{ref}} - p\|$  and control cost,

$$r(x_t, u_t) = -w_p \|e_p\|^2 - w_u \|u_t\|^2 + C_{\text{alive}} \quad (59)$$

where  $w_p$  and  $w_u$  are weighting coefficients and  $C_{\text{alive}}$  is a survival bonus.

**Model Approximation via PyKoopman:** The control-affine linear model required for the Lyapunov constraint was learned using the PyKoopman library [27], a Python package for data-driven approximation of the Koopman operator. We collected a dataset  $\mathcal{D}_{\text{edmd}}$  consisting of 17,000 state transitions  $(e_k, u_k, e_{k+1})$ . Trajectories were generated using a baseline PID controller with added Gaussian exploration noise to ensure sufficient excitation of the state space. We employed a dictionary of observables  $\Psi(e)$  consisting of the state variables themselves concatenated with Radial Basis Functions (RBFs) to capture nonlinearities. The centers of RBFs were determined via k-means clustering on  $\mathcal{D}_{\text{edmd}}$ . The finite-dimensional approximation of the Koopman operator was computed using the EDMD method with Tikhonov regularization ( $\lambda = 10^{-5}$ ) to prevent overfitting,

$$\min_{\mathbf{K}} \|\Psi(E') - \Psi(E)\mathbf{K} - \Psi(U)\mathbf{B}\|_F^2 + \lambda \|\mathbf{K}\|_F^2 \quad (60)$$

The resulting system matrices  $(A, B)$  in the lifted space were validated by comparing the multi-step prediction error against the ground truth safe-control-gym 2D quadrotor environment.

**Lyapunov-constrained SAC and baseline SAC:** Both the baseline Soft Actor-Critic (SAC) and the proposed LC-SAC were implemented using the PyTorch [28] deep learning framework. Actor ( $\pi_\phi$ ): A Multi-Layer Perceptron (MLP) with two hidden layers of 128 units each and ReLU activation. The output layer uses a Tanh activation to map actions to the valid range  $[-1, 1]$ . Critic ( $Q_\theta$ ): A dual-head MLP architecture (Clipped Double-Q Learning) with similar dimensions to the actor. The networks were optimized using Adam. The temperature parameter  $\alpha$  was automatically tuned to maintain a target entropy of  $\bar{\mathcal{H}} = -\dim(\mathcal{A})$ . Lyapunov Constraint: The closed-form CLF matrix  $P$  was computed offline using the `scipy.linalg.solve_discrete_are` [29] solver based on the EDMD matrices. The decay rate  $\eta$  was set to 0.1.

Table I covers the remaining choice of hyperparameters for LC-SAC and baseline SAC training. All experiments were run on a workstation running Ubuntu 24.1 equipped with an NVIDIA ADA 4000 GPU. Results are reported as the average over 5 random seeds to account for stochasticity in training.

TABLE I  
HYPERPARAMETERS LC-SAC AND BASELINE SAC

| Parameters                       | Value              |
|----------------------------------|--------------------|
| Optimizer                        | Adam               |
| Learning Rate                    | $3 \times 10^{-4}$ |
| Batch Size                       | 128                |
| Discount Factor( $\gamma$ )      | 0.99               |
| Replay Buffer Size               | $10^6$             |
| $\tau$ (Polyak averaging)        | 0.005              |
| Lifting Dimension ( $N_{lift}$ ) | 8                  |

## V. RESULTS

We evaluate the proposed Lyapunov-Constrained SAC (LC-SAC) against a baseline SAC controller on quadrotor trajectory tracking in `safe-control-gym`. Appendix A discusses the results and conclusions for EDMD surrogate model. The LC-SAC implementation augments the standard SAC actor update with (i) a Lyapunov decrease penalty computed on the lifted tracking-error state and (ii) a primal-dual Lagrange multiplier update to adaptively enforce the constraint. In particular, the code computes the lifted error  $z = g(e)$  with  $e = x - x_{ref}$ , predicts the next lifted error using the EDMD model  $z^+ = Az + Bu$ , evaluates  $V(z) = z^\top P z$ , and forms the hinge penalty

$$\mathcal{L}_v = \text{ReLU}(V(z^+) - V(z) + \eta V(z)), \quad (61)$$

where  $\eta = 0.001$ , with terminal transitions masked out, and then aggregates the *worst tail* of violations using a top- $k$  (CVaR) mean. The actor objective is

$$\mathcal{L}_\pi = \mathcal{L}_{\text{SAC}} + \lambda(\mathcal{L}_v - \zeta), \quad (62)$$

where,  $\zeta = 1 \times 10^{-6}$  and the multiplier is updated by projected ascent and clamped to a maximum value (0.1).

Figure 3 illustrates the Lyapunov loss over training and its moving average. The raw per-update loss is highly variable early in training (reflecting exploratory actions and frequent constraint violation), followed by a clear reduction and stabilization as learning progresses. The moving-average curve shows a sharp initial drop and then a long plateau at a substantially lower level, indicating that the learned policy increasingly selects actions that reduce predicted Lyapunov violations under the EDMD model. A key reason this signal remains informative (rather than being washed out by averaging) is the CVaR aggregation used in the implementation. Instead of minimizing the batch mean of violations, LC-SAC minimizes the mean of largest violations in the batch (top- $k$ ), focusing learning pressure on rare but severe instability events. Empirically, this behavior is consistent with the observed training dynamics, i.e., the constraint loss decreases in its worst-case tail while occasional spikes persist due to distribution shift and exploration.

Figure 4 compares episode rewards (training) and evaluation rewards (mean  $\pm$  std). Quantitatively, LC-SAC achieves a substantially higher final training performance and more stable evaluation returns. Interestingly, baseline SAC shows a higher

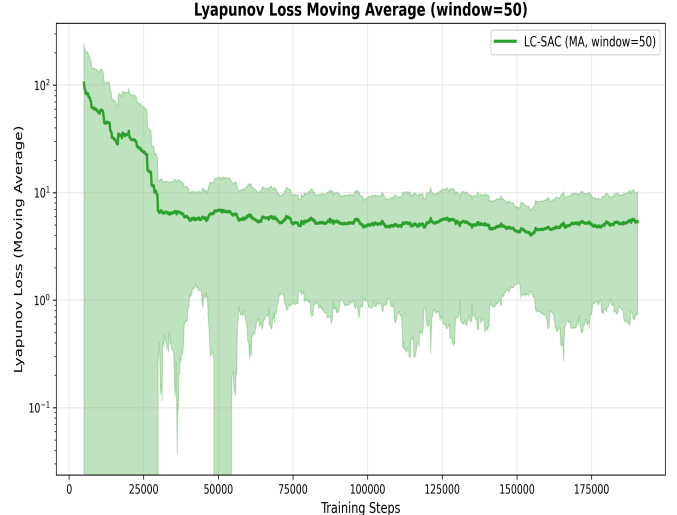


Fig. 3. Lyapunov Loss decay for LC-SAC over 5 trials.

(and far more variable) maximum episode reward compared to LC-SAC. This pattern is typical of unconstrained SAC, occasional lucky rollouts achieve high reward, but performance is not reliably sustained. In contrast, LC-SAC trades off some extreme peak outcomes to achieve significantly better consistent final performance and improved evaluation stability, consistent with a safety-regularized objective.

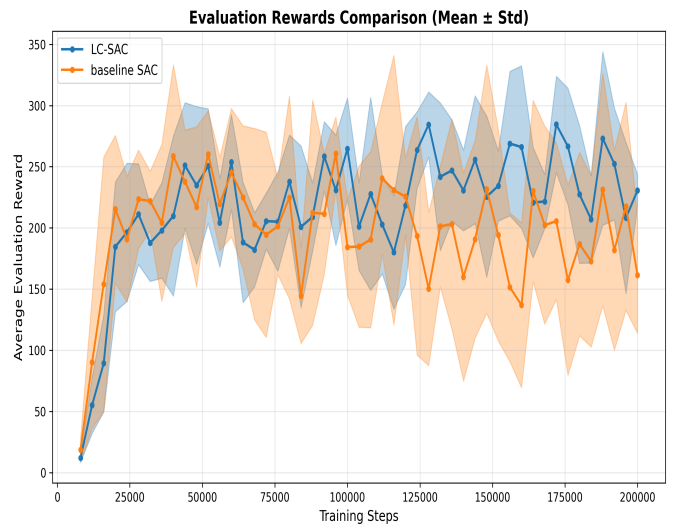


Fig. 4. Average evaluation rewards during training for proposed LC-SAC and baseline SAC.

Figure 5 compares the mean X-Z trajectories and their variance. LC-SAC tracks the reference more consistently, with reduced spread around the mean path. This aligns with the mechanism of penalizing predicted increases in the lifted error energy, actions that would amplify tracking error are discouraged, particularly in the worst-case tail of transitions (via the top- $k$  aggregation). A qualitative but important observation is that the baseline SAC mean trajectory can appear competitive in some segments while still exhibiting larger variance (wider uncertainty band). This explains why baseline

SAC can occasionally reach high peak rewards (high episode maxima) yet under perform in final and evaluation averages, it learns behaviors that are intermittently good but not robust across episodes/trials.

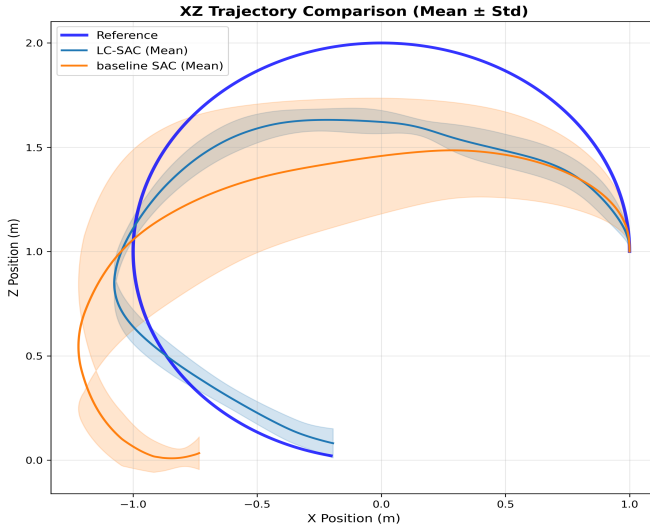


Fig. 5. Mean and Variance trajectory comparison for LC-SAC vs baseline SAC in X-Z plane.

By optimizing a CVaR Lyapunov penalty, LC-SAC directly reduces large, rare violations that typically precede divergence and poor tracking. This mechanism is reflected in the strong decay of the Lyapunov loss early and its lower steady-state level thereafter (Fig. 3). The Lagrange multiplier update increases  $\lambda$  when the Lyapunov loss exceeds the tolerance and decreases it otherwise (via projection and clamping), automatically strengthening constraint pressure in difficult regions while relaxing it in safe regimes. This helps explain why LC-SAC achieves higher final returns than baseline SAC. Once violations reduce, the actor update is effectively closer to standard SAC, allowing reward maximization without persistent over-regularization.

The evaluation statistics in Table II show that LC-SAC not only improves mean return but also significantly reduces trial-to-trial dispersion compared to baseline SAC. This is consistent with learning a policy that is less sensitive to stochasticity (initial conditions, exploration noise, and model mismatch). The Lyapunov penalty is computed using the EDMD one-step prediction  $z^+ = Az + Bu$  rather than the true environment transition, so the loss curves should be interpreted as surrogate-model feasibility. Nevertheless, the simultaneous improvement in real environment rewards and trajectory tracking indicates that the surrogate decrease condition is sufficiently aligned with the true dynamics in the visited region to yield practical stability benefits.

Overall, LC-SAC achieves (i) substantially higher and more reliable final training performance, (ii) higher and significantly more stable evaluation returns, and (iii) improved trajectory tracking consistency in the X-Z plane, while maintaining comparable best-case evaluation performance to baseline SAC. These outcomes are consistent with the proposed design: enforcing Lyapunov decrease on the lifted tracking-error state

using EDMD predictions and concentrating the penalty on worst-case violations through a CVaR loss.

## VI. CONCLUSION

This work presented a Lyapunov-Constrained Soft Actor-Critic (LC-SAC) framework for quadrotor trajectory tracking in `safe-control-gym`, combining offline EDMD-based Koopman lifting with an online primal-dual constrained policy optimization scheme. The nonlinear tracking problem is proposed in an error-state form and EDMD is used to obtain a discrete-time lifted surrogate model. A closed-form quadratic candidate CLF is then constructed by solving the DARE, enabling an efficient and differentiable Lyapunov violation term without training an additional Lyapunov network. During online learning, the actor is trained with a Lagrangian-augmented SAC objective that penalizes one-step Lyapunov increases, while a projected dual update adapted the multiplier to enforce the constraint within a prescribed tolerance.

Empirically, the proposed LC-SAC method demonstrated clear improvements in tracking performance and robustness relative to baseline SAC. While baseline SAC occasionally produced higher maximum episodic returns, its large variance indicated less reliable behavior, whereas LC-SAC delivered tighter performance dispersion and improved trajectory consistency in the X-Z plane. The Lyapunov loss curves further showed a rapid reduction and stabilization over training, consistent with the policy learning to avoid actions that increase the predicted lifted error energy under the EDMD model. Overall, these results support the central claim that incorporating a model-based Lyapunov decrease constraint into maximum-entropy RL can improve safety and stability for trajectory tracking, while preserving the performance benefits of off-policy SAC.

Several directions can strengthen both theoretical guarantees and empirical performance. The Lyapunov constraint is evaluated using the EDMD one-step prediction  $z^+ = Az + Bu$ , and thus provides stability guarantees with respect to the surrogate model, a natural next step is to incorporate explicit model-mismatch bounds and use these bounds to select conservative margins and tolerances. Quadrotor tracking involves actuator saturation, tilt/angle limits, velocity bounds, and obstacle avoidance. Future work should integrate multiple constraints (e.g., control barrier functions or explicit inequality constraints) alongside the Lyapunov decrease condition, and study how to balance competing constraints within the same primal-dual training loop.

## REFERENCES

- [1] S. Gu, L. Yang, Y. Du, G. Chen, F. Walter, J. Wang, and A. Knoll, “A review of safe reinforcement learning: Methods, theories and applications,” *IEEE Transactions on Pattern Analysis and Machine Intelligence*, 2024.
- [2] D. S. Kushwaha and Z. A. Biron, “A review on safe reinforcement learning using lyapunov and barrier functions,” *arXiv preprint arXiv:2508.09128*, 2025.
- [3] T. J. Perkins and A. G. Barto, “Lyapunov design for safe reinforcement learning,” *Journal of Machine Learning Research*, vol. 3, no. Dec, pp. 803–832, 2002.
- [4] Y. Chow, O. Nachum, E. Duenez-Guzman, and M. Ghavamzadeh, “A lyapunov-based approach to safe reinforcement learning,” *Advances in neural information processing systems*, vol. 31, 2018.

TABLE II  
PERFORMANCE SUMMARY FOR QUADROTOR TRAJECTORY TRACKING IN `SAFE-CONTROL-GYM` (MEAN  $\pm$  STD ACROSS TRIALS).

| Metric                              | LC-SAC              | baseline SAC        |
|-------------------------------------|---------------------|---------------------|
| Final training reward (last 10 eps) | $264.06 \pm 30.85$  | $64.27 \pm 0.00$    |
| Max episode reward (training)       | $374.25 \pm 4.13$   | $461.36 \pm 146.49$ |
| Overall episode reward (training)   | $136.99 \pm 166.37$ | $123.06 \pm 161.41$ |
| Convergence episodes                | $570.80 \pm 108.30$ | $620.20 \pm 246.09$ |
| Final evaluation reward             | $230.66 \pm 13.07$  | $161.34 \pm 47.55$  |
| Best evaluation reward              | $331.71 \pm 19.22$  | $323.98 \pm 26.95$  |
| Best eval reward range (min–max)    | [297.47, 355.42]    | [281.09, 350.43]    |

[5] Y. Chow, O. Nachum, A. Faust, E. Duenez-Guzman, and M. Ghavamzadeh, “Lyapunov-based safe policy optimization for continuous control,” *arXiv preprint arXiv:1901.10031*, 2019.

[6] M. Han, L. Zhang, J. Wang, and W. Pan, “Actor-critic reinforcement learning for control with stability guarantee,” *IEEE Robotics and Automation Letters*, vol. 5, no. 4, pp. 6217–6224, 2020.

[7] P. Osinenko, L. Beckenbach, T. Göhrt, and S. Streif, “A reinforcement learning method with closed-loop stability guarantee,” *IFAC PapersOnLine*, vol. 53, no. 2, pp. 8043–8048, 2020.

[8] F. Berkenkamp, M. Turchetta, A. Schoellig, and A. Krause, “Safe model-based reinforcement learning with stability guarantees,” *Advances in neural information processing systems*, vol. 30, 2017.

[9] L. Brunke, M. Greeff, A. W. Hall, Z. Yuan, S. Zhou, J. Panerati, and A. P. Schoellig, “Safe learning in robotics: From learning-based control to safe reinforcement learning,” *Annual Review of Control, Robotics, and Autonomous Systems*, vol. 5, no. 1, pp. 411–444, 2022.

[10] S. Gill and D. Constantinescu, “Off policy lyapunov stability in reinforcement learning,” in *Proceedings of The 9th Conference on Robot Learning*, ser. Proceedings of Machine Learning Research, J. Lim, S. Song, and H.-W. Park, Eds., vol. 305. PMLR, 27–30 Sep 2025, pp. 4093–4102. [Online]. Available: <https://proceedings.mlr.press/v305/gill25a.html>

[11] A. López and D. Fridovich-Keil, “Decomposing control lyapunov functions for efficient reinforcement learning,” in *2025 American Control Conference (ACC)*. IEEE, 2025, pp. 180–187.

[12] A. D. Ames, S. Mattenet, and J. Moeller, “Categorical lyapunov theory ii: Stability of systems,” *arXiv preprint arXiv:2505.22968*, 2025.

[13] H. Khalil, *Nonlinear Systems*, ser. Pearson Education. Prentice Hall, 2002. [Online]. Available: [https://books.google.com/books?id=t\\_dIQgAACAAJ](https://books.google.com/books?id=t_dIQgAACAAJ)

[14] E. D. Sontag, “A ‘universal’construction of artstein’s theorem on nonlinear stabilization,” *Systems & control letters*, vol. 13, no. 2, pp. 117–123, 1989.

[15] S. Meyn, *Control systems and reinforcement learning*. Cambridge University Press, 2022.

[16] T. Haarnoja, A. Zhou, K. Hartikainen, G. Tucker, S. Ha, J. Tan, V. Kumar, H. Zhu, A. Gupta, P. Abbeel *et al.*, “Soft actor-critic algorithms and applications,” *arXiv preprint arXiv:1812.05905*, 2018.

[17] S. Fujimoto, H. Hoof, and D. Meger, “Addressing function approximation error in actor-critic methods,” in *International conference on machine learning*. PMLR, 2018, pp. 1587–1596.

[18] S. L. Brunton, M. Budišić, E. Kaiser, and J. N. Kutz, “Modern koopman theory for dynamical systems,” *arXiv preprint arXiv:2102.12086*, 2021.

[19] M. Korda and I. Mezić, “On convergence of extended dynamic mode decomposition to the koopman operator,” *Journal of Nonlinear Science*, vol. 28, no. 2, pp. 687–710, 2018.

[20] J. C. A. Barata and M. S. Hussein, “The moore–penrose pseudoinverse: A tutorial review of the theory,” *Brazilian Journal of Physics*, vol. 42, no. 1, pp. 146–165, 2012.

[21] I. Mezić, “Spectral properties of dynamical systems, model reduction and decompositions,” *Nonlinear Dynamics*, vol. 41, no. 1, pp. 309–325, 2005.

[22] M. O. Williams, I. G. Kevrekidis, and C. W. Rowley, “A data–driven approximation of the koopman operator: Extending dynamic mode decomposition,” *Journal of Nonlinear Science*, vol. 25, no. 6, pp. 1307–1346, 2015.

[23] R. Freeman and J. Prims, “Control lyapunov functions: new ideas from an old source,” in *Proceedings of 35th IEEE Conference on Decision and Control*, vol. 4, 1996, pp. 3926–3931 vol.4.

[24] M. Sassano, “Policy algebraic equation for the discrete-time linear quadratic regulator problem,” *IEEE Transactions on Automatic Control*, 2024.

[25] C. Tessler, D. J. Mankowitz, and S. Manner, “Reward constrained policy optimization,” *arXiv preprint arXiv:1805.11074*, 2018.

[26] Z. Yuan, A. W. Hall, S. Zhou, L. Brunke, M. Greeff, J. Panerati, and A. P. Schoellig, “Safe-control-gym: A unified benchmark suite for safe learning-based control and reinforcement learning in robotics,” *IEEE Robotics and Automation Letters*, vol. 7, no. 4, pp. 11142–11149, 2022.

[27] S. Pan, E. Kaiser, B. M. de Silva, J. N. Kutz, and S. L. Brunton, “Pykoopman: A python package for data-driven approximation of the koopman operator,” *arXiv preprint arXiv:2306.12962*, 2023.

[28] A. Paszke, S. Gross, F. Massa, A. Lerer, J. Bradbury, G. Chanan, T. Killeen, Z. Lin, N. Gimelshein, L. Antiga *et al.*, “Pytorch: An imperative style, high-performance deep learning library,” *Advances in neural information processing systems*, vol. 32, 2019.

[29] T.-C. Kao and G. Hennequin, “Automatic differentiation of sylvester, lyapunov, and algebraic riccati equations,” *arXiv preprint arXiv:2011.11430*, 2020.

## APPENDIX EDMD SURROGATE MODEL PERFORMANCE

This appendix evaluates the quality of learned EDMD/Koopman surrogate used inside LC-SAC and discusses its implications for Lyapunov constraint. The actor’s stability penalty is computed from a *one-step* prediction in lifted error coordinates:

$$e_t := x_t - x_{\text{ref},t}, \quad z_t := g(e_t), \quad \hat{z}_{t+1} = Az_t + Bu_t, \quad (63)$$

and the candidate CLF is

$$V(z) = z^\top P z, \quad (64)$$

implemented directly in the code via the EDMD observables `lift` and a quadratic form with the DARE-derived  $P$  matrix. Figure 6 (True vs Koopman Prediction) compares true tracking-error trajectories and EDMD one-step predictions for key 2D quadrotor error channels (e.g.,  $e_x$ ,  $e_{\dot{x}}$ ,  $e_z$ ). The curves exhibit near overlap for  $e_x$  and  $e_z$  (reported RMSE  $\approx 0.000$  in the plot legend), and a small but visible discrepancy for the velocity error  $e_{\dot{x}}$  (reported RMSE  $\approx 0.020$ ).

These results indicate that, for the data distribution used to train EDMD, the lifted linear model captures the dominant tracking-error evolution with high fidelity. The slightly larger error on  $e_{\dot{x}}$  is expected: derivative-like states typically have higher bandwidth and are more sensitive to discretization, measurement noise, and unmodeled dynamics. Importantly, LC-SAC requires only *local, one-step* consistency to produce

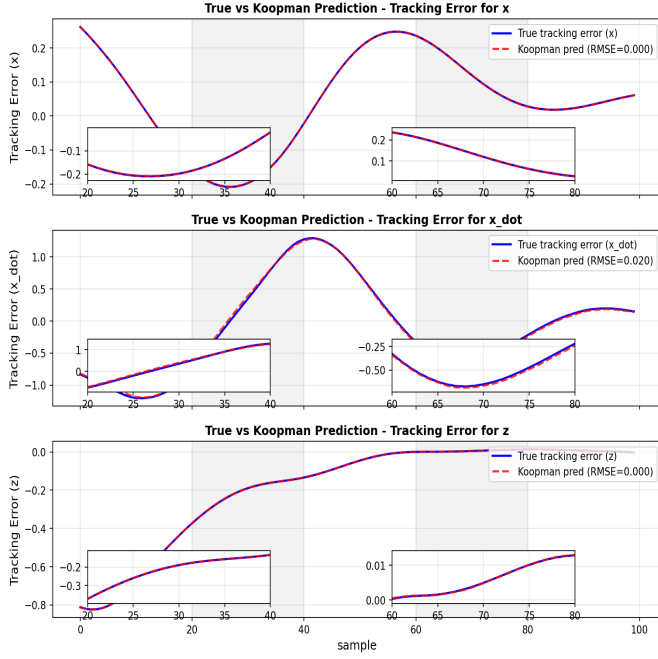


Fig. 6. Tracking error prediction using EDMD for position and velocity in XZ plane.

meaningful gradients for constraint reduction it does not require the EDMD model to remain accurate over long horizons.

The Lyapunov penalty used by LC-SAC is computed by predicting the next lifted error using EDMD and evaluating the change in  $V$ :

$$V_t := V(z_t), \quad V_{t+1} := V(\hat{z}_{t+1})$$

$$\mathcal{L}_v = \text{ReLU}(V_{t+1} - V_t + \eta V_t), \quad (65)$$

where  $\eta$  is the decay rate in the implementation. The predicted step is computed as  $\hat{z}_{t+1} = z_t A^\top + u_t B^\top$  (equivalently  $Az_t + Bu_t$ ), and  $V$  is evaluated via the quadratic form  $z^\top P z$ .

The actor update uses reparameterized actions, so gradients backpropagate through  $u_t \mapsto \hat{z}_{t+1} \mapsto V(\hat{z}_{t+1})$ . Therefore, the constraint provides a useful learning signal if the EDMD map is *locally consistent* in the region visited by the policy. The near-perfect overlap in the prediction plots suggests the model provides a reliable local surrogate—particularly for position-related errors—which aligns well with the observed Lyapunov-loss reduction during training.

The constraint is enforced on  $\hat{z}_{t+1} = Az_t + Bu_t$  rather than the true next error  $z_{t+1} = g(e_{t+1})$ . Hence, the Lyapunov loss reflects *surrogate-model feasibility*. When EDMD is accurate (as suggested by Fig. 6), surrogate decrease tends to correlate well with true decrease; when distribution shift occurs, the penalty remains a conservative regularizer but no longer constitutes a formal guarantee for the true dynamics. This motivates future work on (i) on-policy EDMD updates and (ii) robust margins that incorporate prediction uncertainty. Figure 7 visualizes the DARE-derived matrix  $P$  in the lifted space through a heatmap and its eigenvalue spectrum. The eigenvalues are real and non-negative in the plot, which is consistent with  $P \succeq 0$  as expected from the discrete-time

LQR/DARE solution used to define the quadratic CLF. In addition, the spectrum appears highly *anisotropic*: a small number of large eigenvalues dominate, while several eigenvalues are near zero.

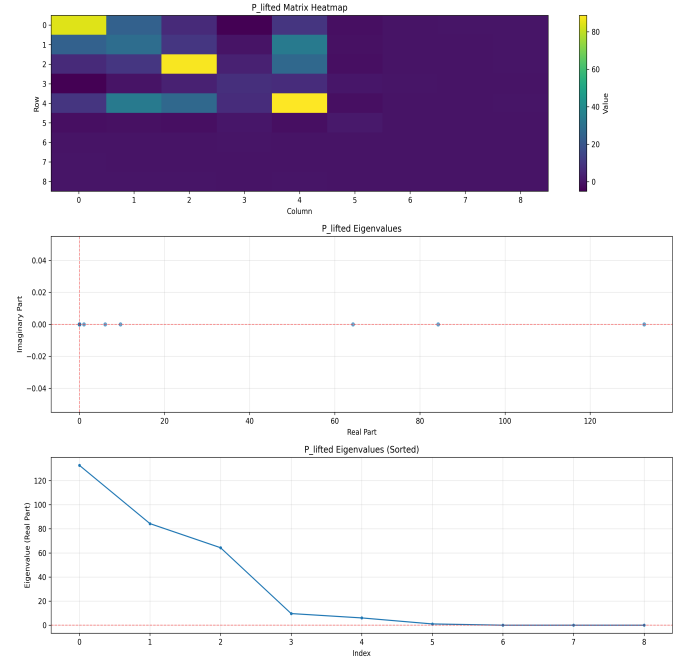


Fig. 7. Eigenvalue analysis for  $P$  matrix computed by solving DARE.

This structure has two practical consequences. Since,

$$V(z) = z^\top P z = \sum_{i=1}^N \lambda_i \xi_i^2, \quad (66)$$

in the eigenbasis  $z = \sum_i \xi_i v_i$ , large  $\lambda_i$  strongly penalize specific lifted directions (often corresponding to task-relevant error modes), while near-zero eigenvalues imply directions that contribute little to  $V$ . This can be beneficial: the CLF emphasizes the most important components of the lifted error for stabilization.

A wide eigenvalue spread implies a large condition number, which can make  $V$  (and thus  $\mathcal{L}_v$ ) sensitive to small modeling errors in heavily weighted directions. In practice, this is mitigated by (a) the hinge structure (penalize only when violated), (b) the dual update that adapts  $\lambda$ , and (c) the CVaR top- $k$  aggregation that targets the most problematic samples. If needed, numerical conditioning can be improved by regularizing the DARE solution (e.g.,  $P \leftarrow P + \chi P I$ ) or by designing  $Q, R$  to avoid excessively ill-conditioned  $P$ . The EDMD plots show strong one-step predictive agreement on the tracking-error channels used by the controller, which supports the use of  $Az + Bu$  as a differentiable surrogate for Lyapunov constraint computation. Combined with a PSD DARE-derived  $P$  and a worst-tail violation objective, the EDMD module provides a computationally efficient and empirically well-aligned stability signal for LC-SAC in the 2D quadrotor tracking task.